Photon-beam lithography reaches 12.5 nm half-pitch resolution

Harun H. Solak,[a] Yasin Ekinci, and Philipp Käser
Laboratory for Micro and Nanotechnology, Paul Scherrer Institute, 5232 Villigen PSI, Switzerland

Sunggook Park
Mechanical Engineering Department, Louisiana State University, Baton Rouge, Louisiana 70803

(Received 31 May 2006; accepted 30 October 2006; published 3 January 2007)

We have printed dense line/space patterns with half-pitches as small as 12.5 nm in a negative-tone calixarene resist using extreme ultraviolet (EUV) interference lithography. The EUV interference setup which is based on transmission diffraction gratings is illuminated with spatially coherent radiation from a synchrotron source. The results show the extendibility of EUV lithography to printing features measuring less than 15 nm in size. We discuss the potential impact of effects such as photoelectron blur and shot noise in high-resolution EUV lithography. © *2007 American Vacuum Society.* [DOI: 10.1116/1.2401612]

I. INTRODUCTION

In order to achieve high-resolution patterning in photolithography, one needs an aerial image with high enough contrast and a photoresist that has the capability to turn this image into a useful pattern. The aerial image resolution depends on the wavelength of the used light in all optical image forming methods, including proximity, projection, and interference methods. Other factors, such as photoelectron blur and shot-noise can also affect the achievable resolution. Previously, Flanders demonstrated patterning of 17.5 nm line/shape (L/S) patterns in polymethylmethacrylate (PMMA) using carbon *K* x rays ($\lambda = 4.5$ nm) by using a proximity technique.[1] The resolution limit of 17.5 nm reached in this study was attributed to the limitations of the used photoresist (PMMA), which lost its integrity at smaller linewidths. Solak *et al.* printed 19 nm L/S patterns in PMMA with extreme ultraviolet (EUV) ($\lambda = 13$ nm) interference lithography.[2] More recently Bloomstein *et al.* used immersion interference lithography to obtain 27 nm L/S patterns in PMMA using UV laser light ($\lambda = 157$ nm).[3] The interference lithography techniques used in the latter two cases offer the advantage of perfect contrast in the aerial image, whereas the same is more difficult to achieve in projection and proximity lithography methods.

As exemplified by the cases that we cited above, PMMA has been by far the most widely used resist for high-resolution lithography. Isolated lines measuring less than 5 nm in width[4] and line/space patterns with periods going down to 32 nm have been obtained in this resist with electron-beam lithography.[5] The highest resolution results obtained with photon lithography that are reviewed above also point to a resolution limit of about 35 nm period for dense patterns in PMMA. This apparent limit does not apply to isolated patterns. In particular, note that the sub-5 nm resolution obtained with e-beam lithography is in the form of a narrow gap (trench) in the resist film, not the width of a resist feature itself.[4] Therefore the structural integrity of a small resist feature is not a concern for such isolated patterns. Calixarene derivatives have recently been introduced as negative-tone electron-beam resists with resolution rivaling or exceeding that of PMMA.[6–8] Isolated features measuring less than 10 nm in width[6,7] and dense dot arrays with periods going down to 29 nm (Ref. 8) have been fabricated in this resist. The ultimate resolution of calixarene resists in photon-beam lithography has not been explored until the present work to the best of our knowledge.

Microelectronics industry has been using photolithography to fabricate integrated circuits with ever decreasing dimensions. This trend has been maintained by a number of developments that include migration to smaller wavelengths in the UV region, image enhancement through phase shifting and proximity correction techniques, use of immersion liquids, and better process control. EUV lithography at a wavelength of ~ 13.5 nm is considered as one of the leading candidates for continuation of this miniaturization trend. In order to be an effective lithographic solution, EUV technology needs to provide a resolution of at least 22 nm or better, as measured by the half-pitch of dense line/space-type patterns. Therefore, there is a need to explore and understand the ultimate limits of resolution achievable at this wavelength.

Here we present the fabrication of L/S patterns with periods as small as 25 nm in a calixarene resist using EUV interference lithography. The experimental processes and the resulting patterns are presented in the following sections along with a discussion of factors that influence the resolution.

II. EXPERIMENT

The EUV experiments were performed at the XIL beamline of the Swiss Light Source. This beamline delivers a spatially coherent EUV beam to illuminate a transmission diffraction grating-based interferometer.[9] The period of the interference fringes formed by this interferometer is equal to one-half of the period of the diffraction gratings. This "demagnification" factor of 2 between the mask and the fringe pattern significantly helps with the fabrication of the required

[a]Electronic mail: harun.solak@psi.ch

masks for obtaining high-resolution patterns. The gratings are patterned on thin silicon nitride membranes using electron-beam lithography, as we have previously reported.[10] In particular, the 12.5 nm L/S patterns obtained in this study required the patterning of 25 nm L/S patterns on the mask. For the experiments reported here, the beamline was tuned to provide a beam with a central wavelength of 13.4 nm and a spectral width of about 2%–3%. The spectral width varies with the settings of the source which consists of two independent undulators in series. No effort was made to measure or control this parameter in the experiments reported here as it is deemed to be largely inconsequential for the achromatic, grating-based interferometer.

Calixarene resist (*p*-chloromethyl-methoxy-calix[4] arene, TEBN-1 from Tokuyama Corp., Japan) was spin coated onto substrates, which were either Si wafers coated with a thin film of Cr (10–20 nm thick) or Si wafers primed with hexamethyldisilazane in a vacuum oven. The thickness of the calixarene resist was 25 nm. The resist solution was used as received from the supplier without further dilution. After baking on a hot plate at 110 °C for 60 s, the samples were exposed with EUV fringe patterns with periods in the 25–50 nm range. The patterns were developed in isopropyl alcohol (IPA) for times ranging from 30 to 120 s. Top-down and cross-section images of the developed patterns were obtained with a scanning electron microscopy (SEM).

Contrast and sensitivity of the calixarene resist were measured using open frame exposures at the same beamline. After development, the remaining resist thickness was measured using a mechanical profilometer on one of the edges of the uniformly exposed area. The beam flux is measured by a photodiode and the exposure dose is controlled by a computer controlled exposure shutter. For comparison, contrast curves for PMMA were obtained using the same method. PMMA films with 600 K molecular weight were spin coated onto Si wafers for this purpose. The exposed PMMA films were developed in a 1:3 methyl isobutyl ketone: isopropyl alcohol (MIBK:IPA) solution for 45 s using a spray developer. The thickness of the as deposited PMMA film was 60 nm.

III. RESULTS AND DISCUSSION

Contrast curves for the calixarene and PMMA resists are shown in Fig. 1. The processing conditions and the sensitivity and contrast values obtained from the curves are listed in Table I, which shows that calixarene is four to five times less sensitive than PMMA for EUV exposures. Both resists have similar contrast. This result meant correspondingly longer exposure times for calixarene, which did not reach a level that affected the feasibility of the experiments both in terms of the required times and potential exacerbation of mechanical drift effects.

Top-down SEM images of line/space patterns in calixarene with half pitches in the 20–12.5 nm range are shown in Fig. 2. The samples were inspected directly after development without the deposition of a conducting film. Unlike PMMA, calixarene is stable under the electron beam which

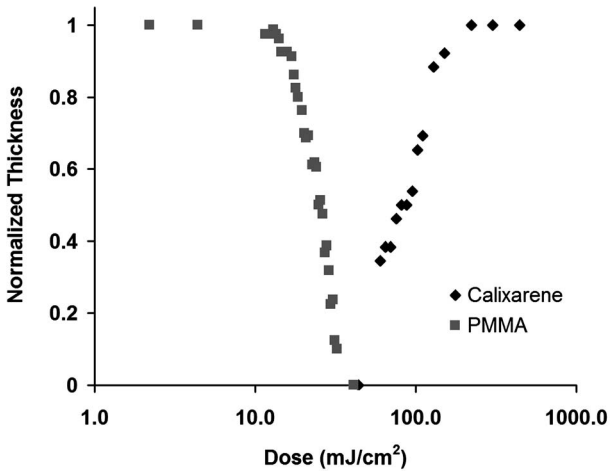

FIG. 1. Contrast curves for PMMA and calixarene resists.

facilitates the imaging of the nanometer-scale features seen here. The lines are continuous and have well-defined edges. The faint structures that can be seen between the lines are due to the grains of the Cr film on the substrate. At the highest resolution level of 12.5 nm we observe occasional bridging between the lines. Isolated lines measuring less than 10 nm in width[6,7] and dense dot arrays with about 29 nm nearest neighbor distance[8] have been produced in this resist with e-beam lithography. However, to our knowledge 25 nm pitch patterns have not been reported previously for this resist. Therefore, the inherent limit of dense line resolution remains to be an open question. In the present study, the highest resolution patterns that we tested had a pitch of 25 nm, which is determined by the resolution (50 nm pitch) of the diffraction gratings that were available to us. Cross-section images of 16.25, 17.5, and 20 nm half-pitch gratings in Fig. 3 show fully cleared spaced and sharp profiles with apparently vertical side walls. In particular, no top loss was observed. In the extreme ultraviolet interference lithography (EUV-IL) setup, dose control is achieved by measuring the dose that is incident on the mask. The dose on the wafer depends on the efficiency of the diffraction gratings, which has not been measured for the gratings used in this study. In most cases, the diffraction efficiency changes between gratings of different periods due to differences in the duty cycle and the etch profile.

For comparison, top-down SEM images of lines printed in PMMA using EUV-IL are shown in Fig. 4. A thin Au film was sputtered onto the PMMA patterns to avoid charging during the SEM inspection. The degradation of line quality is apparent in these images as the half-pitch drops below 20 nm. The low contrast in the 15 nm half-pitch image is likely to be due to significant top loss in this resist.

The image contrast in EUV interference lithography can be influenced by a number of factors. First of all, the transverse coherence length of the beam illuminating the interferometer has to be much larger than the distance between the two gratings that generate the interfering beams. This is guaranteed in our setup by the use of a pinhole that spatially

TABLE I. Processing parameters and measured sensitivity and contrast values for PMMA and calixarene resists exposed with EUV light. D_i and D_f stand for the doses at which the change in remaining resist thickness begins and ends. D_f value for calixarene was determined as the dose at which 80% of the original thickness remained in the exposed area.

Resist	Thickness (nm)	Development	D_i (mJ/cm^2)	D_f (mJ/cm^2)	Contrast
PMMA	60	1:3 MIBK:IPA, 45 s	14	36	2.4
Calixarene	25	IPA, 30 s	44	120	2.3

filters the beam. In addition, the two interfering beams should have roughly equal intensity in order to form a fringe pattern with perfect contrast. This is not expected to cause any significant reduction in contrast except when there is a severe inequality in beam intensities. For example, a 20% difference in intensity will result in a less than 1% reduction in modulation of the aerial image. We have measured the relative intensity of the beams by using a soft x-ray charge coupled device camera which showed that the beam intensities were essentially equal.

Other factors that can affect the quality of the recorded image include mechanical vibrations and drift, scattering of EUV light from the mask, and blurring due to photoelectrons generated in the resist, substrate, or the mask. Although not explicitly measured, the resolution and quality of the obtained patterns suggest that these factors do not influence the resolution down to the 12.5 nm level. Scattering of light due to roughness in the mask pattern can add an incoherent or a coherent background depending on the spatial frequency of the roughness, temporal coherence of the beam, and other geometrical parameters of the interferometer. Spatial coherence does not come into play as the whole mask is assumed to be illuminated coherently, i.e., there are no coherence patches over which one can perform an averaging operation. The coherent background would manifest itself in the form of a speckle pattern that can be particularly troublesome due to the variations it would introduce into the aerial image. Scattering from the mask and its influence on patterning need to be understood through theoretical and experimental studies, which are beyond the scope of this article. The potential effects of photoelectrons on resolution in EUV lithography can become an important issue as the resolution goes down to the 10 nm level and below. Primary electrons that have energy close to the photon energy of about 92.5 eV are not expected to cause significant blurring as their mean free path is much below 1 nm in all materials.[11] However, secondary electrons with energy below about 20 eV can have significantly longer range on the order of several nanometers. Recent experiments that looked at photoemission from EUV optics surfaces as a function of carbon deposit thickness have found that the secondary electron emission from the optics (substrate) surface essentially diminishes after a deposit thickness of about 1 nm.[12] Therefore, we can expect the photoelectron blur not to be a cause for concern in EUV lithography for resolution in the 10 nm range, which is born out by our experimental results.

Shot noise, which arises due to the low number of photons that is required to expose small areas in resist, has long been discussed as a cause of linewidth and line-edge roughness (LER) in EUV lithography.[13–15] As we achieve sub-15 nm resolution, it is worth examining whether we should expect this effect to present itself in the patterns that we obtained. For this purpose we simulated the two-dimensional distribution of absorbed energy in the resist. Figure 5 shows particular realizations of the absorbed energy distribution due to random photon impingement events. In these calcula-

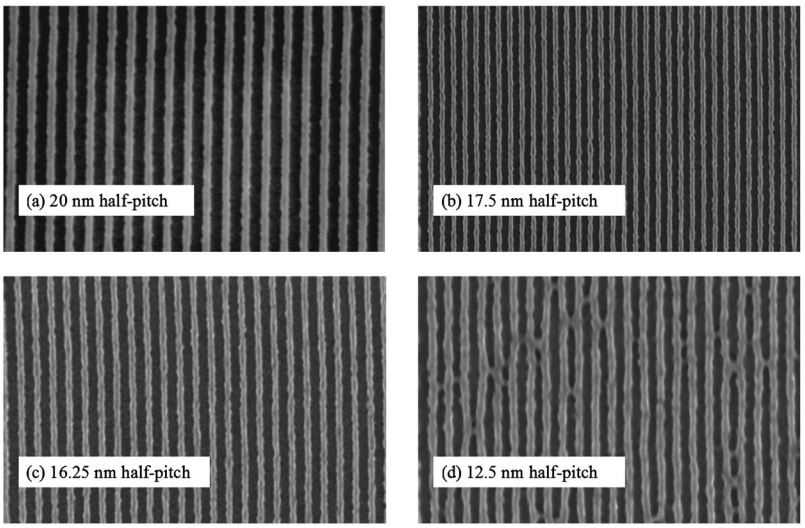

FIG. 2. Top-down SEM micrographs of line/space patterns in calixarene with half-pitches of (a) 20 nm, (b) 17.5 nm, (c) 16.25 nm, and (d) 12.5 nm.

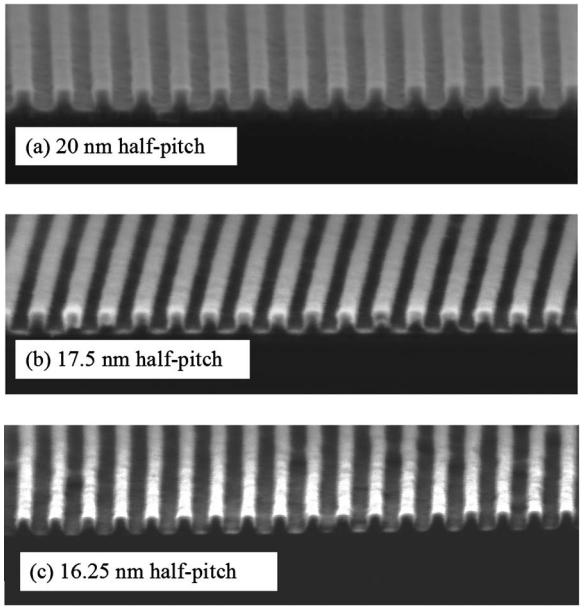

FIG. 3. Cross-section SEM images of calixarene patterns with half-pitches of (a) 20 nm, (b) 17.5 nm, and (c) 16.25 nm.

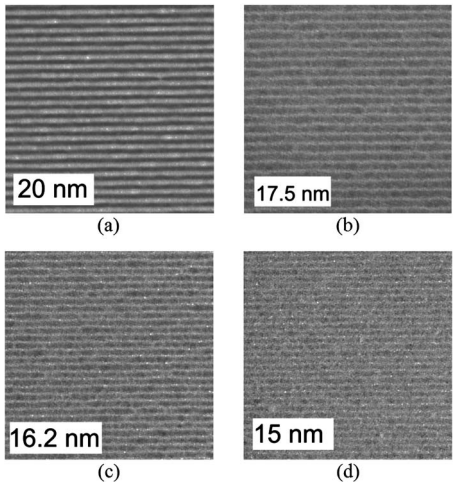

FIG. 4. Top-down SEM micrographs of line/space patterns in PMMA with half-pitches of (a) 20 nm, (b) 17.5 nm, (c) 16.25 nm, and (d) 15 nm. The thickness of the PMMA film is 25 nm.

tions, the photoresist is assumed to absorb 50% of the incident light intensity. In addition, each absorbed photon is assumed to deposit energy around the point of impact with a Gaussian distribution with a standard deviation of $\sigma=1$ nm. This range of impact is reasonable if we only consider the range of secondary electrons, but it does not account for effects such as the diffusion of photoacid in a chemically amplified resist. Furthermore, the model says nothing about other chemical and physical processes that are involved in the recording of the latent image in a photoresist or in the dissolution process, which might need to be considered at a molecular level due to the small size of the features that are under consideration here. The three-dimensional nature of the problem is also neglected even though the impact of a single photon absorption event is not likely to extend through the full thickness of the film. The intensity distribution (without the effect of shot noise) was assumed to be sinusoidal and have perfect contrast, as we expect in an interference setup. Results are shown in Fig. 4 for a half-pitch of 12.5 nm and three different dose-to-size values of 10, 100, and 400 mJ/cm^2. The expected resist images shown in the bottom row of Fig. 5 were found by applying a 50% threshold to the calculated intensity distributions. This simple model predicts significant shot-noise induced line-edge roughness for 10 mJ/cm^2 exposure dose and essentially smooth lines for 400 mJ/cm^2. Therefore, the low sensitivity of the calixarene resist means (120 mJ/cm^2) that the LER that we observe in the SEM images in Fig. 2 is likely to be due to a different origin than shot noise. More experiments on different resists and with different grating masks are required to ascertain the actual origin, which could be related to the photoresist (process) itself or deterministic (nonstatistical) variations in the image that could result from scattering from the mask, as we discussed before.

IV. CONCLUSIONS

The EUV response of a negative-tone calixarene resist has been characterized in terms of its sensitivity and resolution. The results show that 12.5 nm dense line/space patterns are printable with EUV exposures. Photoelectron related blur does not seem to have a significant impact on resolution down to the 12.5 nm level. The EUV interference technique that we used provides ample resolution for testing of new photoresist materials that are being developed for microelectronics production at the 22 nm node and below. Remark-

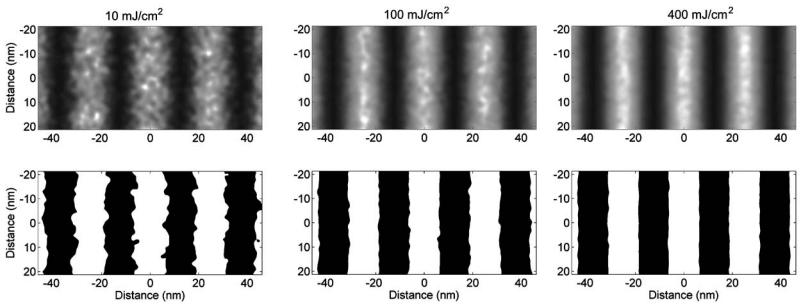

FIG. 5. Top row: simulated intensity distribution for 12.5 nm line/space patterns for exposure doses of 10, 100, and 400 mJ/cm^2. Bottom row: Binary images obtained by applying a threshold to the intensity distributions shown above. The binary images serve as a simple approximation to developed images in a photoresist.

ably, for the first time since the introduction of the e-beam method, a photon based technique rivals e-beam lithography in terms of pattern resolution. Applications that require high-resolution, dense patterns can benefit from this development.

ACKNOWLEDGMENTS

The authors thank F. Glaus, B. Haas, and J. Lehmann for making the Si_3N_4 mask blanks and A. Weber for help with the thin film coatings. Part of this work was performed at the Swiss Light Source, Paul Scherrer Institute, Villigen, Switzerland.

[1]D. C. Flanders, Appl. Phys. Lett. **36**, 93 (1980).
[2]H. H. Solak, D. He, W. Li, S. Singh-Gasson, F. Cerrina, B. H. Sohn, X. M. Yang, and P. Nealey, Appl. Phys. Lett. **75**, 2328 (1999).
[3]T. M. Bloomstein, T. H. Fedynyshyn, I. Pottebaum, M. F. Marchant, S. J. Denault, and M. Rothschild, J. Vac. Sci. Technol. B **24**, 2789 (2006).
[4]S. Yasin, D. G. Hasko, and H. Ahmed, Appl. Phys. Lett. **78**, 2760 (2001).
[5]S. Yasin, D. G. Hasko, and H. Ahmed, Microelectron. Eng. **61–62**, 745 (2002).
[6]J. Fujita, Y. Ohnishi, Y. Ochiai, and S. Matsui, Appl. Phys. Lett. **68**, 1297 (1996).
[7]M. Ishida, J. Fujita, T. Ogura, Y. Ochiai, E. Oshima, and J. Momoda, Jpn. J. Appl. Phys., Part 1 **42**, 3913 (2003).
[8]S. Hosaka, H. Sano, K. Itoh, and H. Sone, Microelectron. Eng. **83**, 792 (2006).
[9]H. H. Solak, J. Phys. D **39**, R171 (2006).
[10]H. H. Solak, C. David, J. Gobrecht, V. Golovkina, F. Cerrina, S. O. Kim, and P. F. Nealey, Microelectron. Eng. **67–68**, 56 (2003).
[11]*Photoemission in Solids I*, edited by M. Cardona and L. Ley (Springer, New York, 1978).
[12]J. Hollenshead and L. Klebanoff, J. Vac. Sci. Technol. B **24**, 64 (2006).
[13]D. van Steenwinckel and J. H. Lammers, J. Vac. Sci. Technol. B **24**, 316 (2006).
[14]G. M. Gallatin, F. A. Houle, and J. L. Cobb, J. Vac. Sci. Technol. B **21**, 3172 (2003).
[15]P. M. Dentinger, L. L. Hunter, D. J. O'Connell, S. Gunn, D. Goods, T. H. Fedynyshyn, R. B. Goodman, and D. K. Astolfi, J. Vac. Sci. Technol. B **20**, 2962 (2002).